Experimental Study on the Static and Fatigue Performances of GFRP-Timber Bolted Connections

Chao Wu [1,2], Zixiao Zhang [1,4], Li He [3] and Lik-ho Tam [1,*]

[1] School of Transportation Science and Engineering, Beihang University, 37 Xueyuan Road, Beijing 100191, China
[2] Department of Civil and Environmental Engineering, Imperial College London, South Kensington Campus, London SW7 2AZ, UK
[3] School of Ecology and Environment, Beijing Technology and Business University, 33 Fucheng Road, Beijing 100048, China
[4] Longfor Group Holdings Limited, 8 Beiyuan Road, Beijing 100012, China

**Corresponding author. E-mail: leo_tam@buaa.edu.cn*

Abstract

Steel plate connection is popular in modern timber structures. However, the steel plate may be subjected to corrosion issue due to the presence of moisture in timbers. This paper proposes to replace steel plate with glass fiber reinforced polymer (GFRP) plate for connecting timber elements, so that the durability of the timber structure is expected to be improved. An experimental study is presented on the static and fatigue performances of the proposed GFRP-timber bolted connections. Variables including bolt diameter, number of bolt rows, number of bolt columns were selected to understand their effects on the static and fatigue behaviours of the connections. Failure modes, load-displacement curves, static bearing capacities, fatigue lives, stiffness degradations of the GFRP-timber bolted connections were reported. The residue bearing capacities of the connections were tested after the fatigue loading tests to assess the fatigue effect on the connection static behaviour. This study contributes to the understanding of the mechanical behaviour of GFRP-timber bolted connections.

KEYWORDS: Bolted connection; GFRP; Timber; Mechanical properties; Fatigue

1. Introduction

Timber has attracted increasing attention in building constructions in recent years as a low carbon material [1, 2]. The timber elements are usually connected with steel plate through bolting which is easy to install and disassemble [3-9]. One issue with this connection is steel corrosion due to the presence of moisture in timber, which significantly affects the durability of the timber structures [10, 11]. In addition, due to the good thermal conductivity of steel plate, the steel plate connections reduce the thermal insulation performance of the building. Glass fiber reinforced polymer (GFRP) is an emerging construction material of light weight, corrosion resistance, and low thermal conductivity [12-20]. It is possible to mitigate the issues of steel plate connections of timber structure by replacing steel plate with GFRP composite.

However, there is very limited study on the GFRP-timber bolted connections. Most existing studies in the literature focus on all FRP connections, all timber connections, or steel-timber connections. Yan et al. [21] reported that the bolt tightening torque could significantly reduce the bolt hole bearing strength of FRP plate connection. Starikov and Schon [23, 24] studied the mechanical properties of FRP connections with multiple bolts. The experimental results showed that the load was not uniformly shared between bolts, and in most cases, the outermost bolts carried much higher load. Similar results were also reported by in other studies [25, 26]. Wu et al. [27] reported a comparative study on the static and fatigue properties of GFRP plate connections with either ordinary bolts or blind bolts. Lawlor et al. [28] reported that the fatigue performance of FRP bolted connections would decrease if the bolt hole clearance was large. Persson et al. [29] ranked the key factors affecting the bearing capacity and fatigue life of FRP plate connections by importance. They found that the ratio of bolt diameter to specimen width, bolt type and bolt hole diameter are the most influencing factors. Abdelkerim et al. [31] studied FRP plate connections with either stainless steel bolts or FRP bolts. They found that the stainless steel bolts could be completely replaced by FRP bolts without affecting the static and fatigue properties of the connections. Jensen and Quenneville [5] and Jockwer et al. [33] studied the effects of bolt end distance and bolt pitch distance on the mechanical properties of steel-timber bolted connections. The results showed that in order to ensure a ductile failure, bolt arrangement should satisfy the requirements in the design specifications. Yurrita et al. [34] reported that Eurocode 5 [35] was too conservative when predicting the mechanical properties of the steel-timber bolted connections. Mohammad and Quenneville [9] studied the influence of the number of bolts and bolt diameter on the mechanical properties of steel-timber bolted connections, and proposed a design formula of bearing capacity. Jorissen [36] studied the influence of bolt pitch distance, bolt end distance, number of bolt rows and number of bolt columns on the mechanical properties of timber bolted connections. The predicted bearing capacities using the design formula by EC5 [35] agreed well with the experimental results.

The authors of the current paper reported an experimental study on the static behaviors of the GFRP-timber bolted connections [37]. Effects of key parameters were studied including bolt diameter, number of bolt rows, number of bolt column and bolt pitch distance. A design formula was proposed to predict the bearing capacity of the connection based on Eurocode 5 [35]. As a subsequent study, this paper presents a further investigation on the static and fatigue behaviors of GFRP-timber bolted connections. The hypothesis of this study is that GFRP-timber bolted connections can have similar mechanical performance to the conventional steel-timber connections. Four key variables were considered, including bolt diameter, number of bolt rows, number of bolt columns and the material of connecting plates. As for the static tests, the failure modes, load-displacement curves and bearing capacities were reported. As for the fatigue tests, the failure modes, stiffness degradation curves and fatigue lives were reported. This paper contributes to the understanding of static and fatigue behaviors of the GFRP-timber bolted connections and to the future development of relevant design guidelines.

2. Experimental Program

2.1. Materials

The GFRP plates are made from pultrusion and have a thickness of 2.2 mm. They were provided by Nanjing Exel Composites Co. Ltd. According to ASTM D 3039 [38], the elastic modulus and tensile strength in the pultrusion direction were measured. According to ASTM D 3518 [39], off-axial tensile test was carried out and the in-plane shear strength at 45° was measured. According to ASTM D 3171 [40], the fiber mass fraction and fiber composition were characterized. The fiber architecture of the GFRP plate consisted of three layers, the middle layer was unidirectional roving, which was sandwiched by two outer layers of surface mats. The average fiber mass fraction was 62.44%, of which unidirectional fibers accounted for about 70%. The bolt hole bearing capacity of the GFRP plate was tested according to ASTM D 5764 [41]. The measured material properties are listed in Table 1.

The timber used in this paper was pine wood, and the longitudinal direction of the timber plates was aligned with the wood grain direction. The absolute moisture content and density of the timber were 7.21% and 469kg/m3 respectively which were measured according to ASTM D 4442 [42] and D 2395 [43]. The timber plates had a width of 140 mm and a thickness of 22 mm. According to ASTM D 3039 [38], the elastic modulus and tensile strength of the timber plate along the grain direction were measured. The bearing capacity of the bolt hole in the timber plate was tested according to ASTM D 5764 [41]. The measured material properties are listed in Table 1.

The bolts used in this paper were 70 mm long hexagon 304 stainless steel common bolts provided by Tianhe Hardware Company. The minimum tensile strength of the bolt was 700MPa, equivalent to Grade A bolt as specified in ASTM A307 [44]. Galvanized gaskets of 1.75 mm thick are used.

Table 1. Mechanical properties of GFRP and timber

Materials	Longitudinal/grain direction		In-plane shear strength (MPa)	Bolt hole bearing strength (MPa)		
	Elastic modulus (GPa)	Tensile strength (MPa)		10 mm	14 mm	18 mm
GFRP	20.41	347.54	43.77	131.24	98.43	98.08
Timber	7.42	27.36	NA	36.67	37.61	27.55

2.2. Specimen design

GFRP-timber bolted connections were prepared, i.e. one timber plate was sandwiched by two external GFRP plates, as shown in Fig. 1. Two steel fixtures were designed in order to install the specimen on the loading machine. One steel fixture was connected to the two external GFRP plates, and the other steel fixture was connected to the timber plate as shown in Fig. 1. When the specimen was installed on the loading machine, the two steel fixtures can be mounted on to the clamps. The two fixtures were connected to the specimen using bolts.

The schematical drawing of the specimen is shown in Fig. 1 The area of interest is marked as “observation section” in Fig. 1 (three bolts in the figure for demonstration purpose). For the actual specimens, the bolt diameter, number and arrangement of bolts in the observation section were changed according to the testing variables (discussed below). The two steel fixtures for clamping the specimen were designed in a way so that the failure would only occur within the observation section. The longitudinal direction of the specimen was aligned in the grain direction of the timber plate as well as in the pultrusion direction of the GFRP plates. In Fig. 1, e_t is the distance from the bolt center to the end of the timber plate. e_{frp} is the distance from the bolt center to the end of the GFRP plate. p is bolt pitch distance.

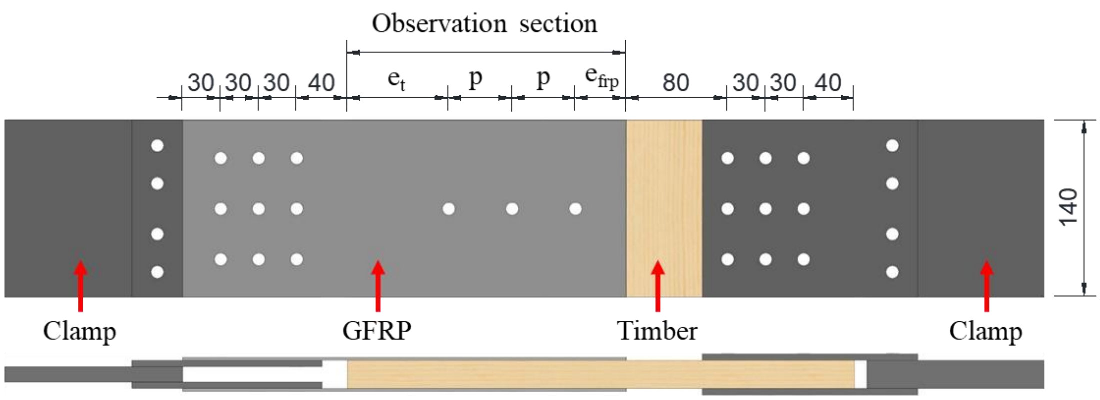

Fig. 1. Schematic of a GFRP-timber connection (plan view and side view)

In this paper, four key variables, including bolt diameter (d), number of bolt rows (n), number of bolt columns (m) and connecting plate material (GFRP plate or steel plate), are studied. For any connections with multiple bolts, the bolts along the tension/longitudinal direction is called bolt column, and the bolts perpendicular to the tension direction is called bolt row. The number of bolts in each column is represented by n_c.

According to these four key variables, the GFRP-timber bolted connections were divided into three groups, namely bolt diameter group, bolt row number group, bolt column number group. In addition, connections with GFRP plates replaced with steel plates were also prepared as control group so that the performance of GFRP-timber connection can be compared with the conventional steel-timber connection. The specimens and their details are presented in Table 2. For each specimen in Table 2, two identical connections were tested for repeating purpose. The name of specimen has three parts, i.e. A-BC. 'A' stands for the connection material with 'G' for GFRP plate and 'S' for steel plate. 'B' represents the group of specimen with 'D' for bolt diameter group, 'N' for bolt row number group and 'M' for bolt column number group. 'C' means the variable value of the corresponding group. For example, "G-D10" represents a specimen with GFRP plates in the bolt diameter group with a bolt diameter of 10 mm. For specimens under fatigue loading, another number is added at the end of the specimen name which refers to the fatigue ratio. For example, "G-D10-08" represents the specimen G-D10 under fatigue loading with a fatigue ration of 0.8.

Currently there is no design specifications available particularly for GFRP-timber connections. Therefore, international design specifications for timber structures and GFRP structures [35, 45] were referred to when designing the connections in this study. According to Eurocode 5 of timber structures [35], it specifies that (1) the minimum distance between bolt holes, center-to-center, should be no less than five times the diameter of the hole; (2) the minimum end distance, center-to-end, should be no less than seven times the diameter of the hole or 80 mm; and (3) the minimum side distance, center-to-side, should be no less than three times the diameter of the hole. According to the design specifications of GFRP bolted connections, Dittenber and Rao [45] proposed that (1) the minimum distance between holes, center-to-center, should be no less than four times the diameter of the hole; (2) the minimum end distance, center-to-end, should be no less than four times the diameter of the hole; and (3) the minimum side distance, center-to-side, should be no less than 1.5 times the diameter of the hole. Therefore, the connections in this paper were designed to satisfy the requirements for both timber and GFRP structures. Fig. 2 shows the designs of typical specimens in different groups.

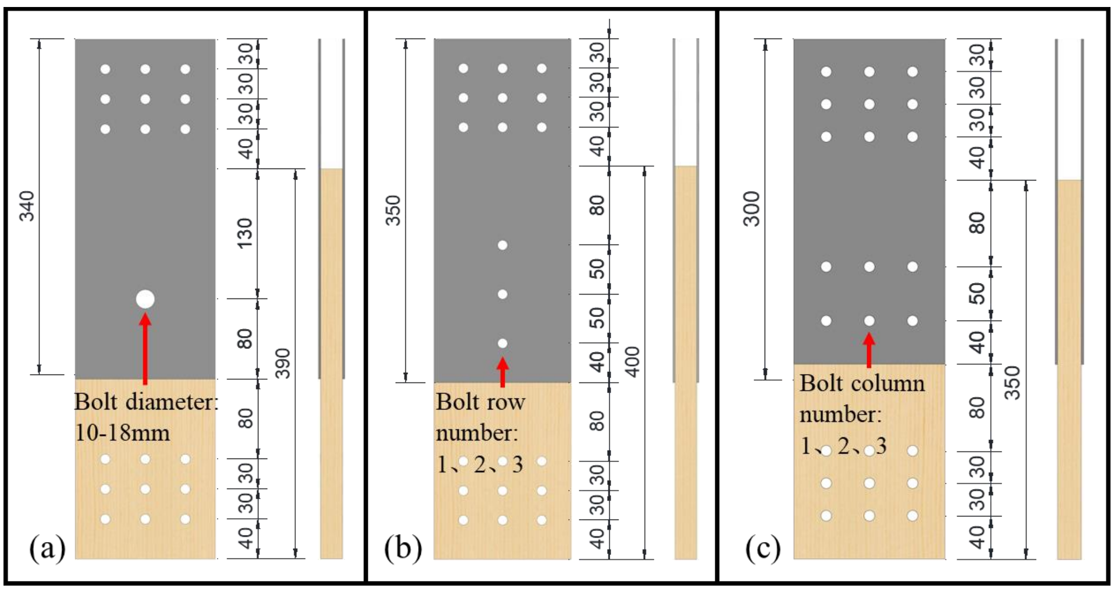

Fig. 2. Dimensions of specimens in the (a) bolt diameter group, (b) bolt row number group and (c) bolt column number group

The specimens in the bolt diameter group in Fig. 2(a) had only one bolt of three different bolt diameters, i.e. 10 mm, 14 mm and 18 mm respectively. The specimens in the bolt row number group in Fig. 2(b) had one column of bolts, and row number changed from 1 to 3. All bolts had a diameter of 10 mm. The specimens in the bolt column number group in Fig. 2(c) had bolt rows, and the bolt column number was 1, 2 and 3 respectively. All bolts were 10 mm in diameter. It should be noted that it is not ideal for GFRP connections have only one bolt. However, the specimens in bolt diameter group were designed to have only one bolt for two reasons. Firstly, this bold diameter group is served as a control group so that to compare with the other groups with multiple bolts. In this way, a better understanding of bolt group effect can be obtained, i.e. connection with two bolts may not necessarily double the capacity of the connection with single bolt. The second reason is that the connection with only one bolt is easier for the observation of the effect of bolt diameter.

When the specimens were manufactured, the bolt holes were drilled by 1 mm larger than the bold diameter. This is to consider the installation tolerance of multiple bolt connections. The bolt holes on GFRP plate and timber plate were drilled using a digital controlled drilling machine with an accuracy of ± 0.01 mm. All specimens were assembled with ease and no forcing was used to tighten the bolts, indicating that the bolt hole tolerance was sufficient.

Table 2. Specimens and detail parameters

Group	**Specimen**	***d*** **(mm)**	$\boldsymbol{n_c}$	***m***	***p*** **(mm)**	$\boldsymbol{e_t}$ **(mm)**	$\boldsymbol{e_{frp}}$ **(mm)**
Bolt diameter group	G-D10	10	1	1	-	130	80
	G-D14	14	1	1	-	130	80
	G-D18	18	1	1	-	130	80
	S-D18	18	1	1	-	130	80
Bolt row number group	G-N1	10	1	1	-	80	40
	G-N2	10	2	1	50	80	40
	G-N3	10	3	1	50	80	40

	S-N3	10	3	1	50	80	40
Bolt column number group	G-M1	10	2	1	50	80	40
	G-M2	10	2	2	50	80	40
	G-M3	10	2	3	50	80	40
	S-M3	10	2	3	50	80	40

Note: d is bolt diameter; n_c is the number of bolts in each column; m is the number of bolt columns; p is bolt pitch distance; e_t is the distance from the bolt center to the end of the timber plate; e_{frp} is the distance from the center of the bolt to the end of the GFRP plate, as shown in Fig. 1.

2.3. Experimental set up and loading programs

All tests were carried out on an INSTRON 8802 loading machine as shown in Fig. 3. The displacement of the connections was measured by a linear variable differential transformer (LVDT). The gauge length was from the upper clamp to the end of the GFRP plate.

Two loading scenarios were performed including static tensile loading and fatigue loading. For static loading, the specimens were tested with a displacement control at a speed of 2 mm/min until failure. The load and displacement were recorded at 10Hz frequency. For fatigue loading, the load was applied with a load control at a loading frequency of 10Hz. The fatigue load ratio was 0.1, which was the ratio between the minimum tensile load $F_{\min}$ and the maximum tensile load $F_{\max}$. The specimens were loaded until failure or up to 2 million cycles. The load and displacement were recorded at 80Hz frequency in fatigue testing. For specimens which did not fail after fatigue loading, they were tensioned to failure to obtain their residue loading capacities.

The moisture content of the timber plate of each specimen was measured immediately after the test. This is because timber properties are sensitive to moisture content and the data were useful to understand the static and fatigue loading behaviour of the connections.

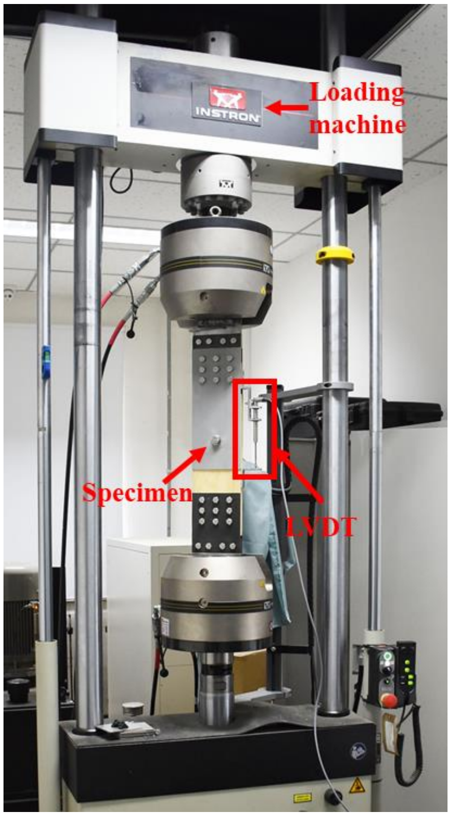

Fig. 3. Experimental set up

3. Experimental Results of Static Tension Tests

3.1. Failure modes

Typical failure modes of specimens in static testing are presented in Fig. 4. Both specimens with GFRP plates and steel plates are compared. For the specimens in the bolt diameter group, they only had one bolt of different bolt diameters. Most specimens showed the bearing failure of the bolt hole in the timber plate as shown in Fig. 4(a), i.e. the bolt gradually squeezed and slide in the hole and the timber hole was crushed and indented. Eventually the timber plate split due to extensive hole crushing. Connections with steel plates showed similar failure modes as shown in Fig. 4(b).

For the specimens in the bolt row number group, they all had the same bolt diameter of 10 mm and the row number changed from 1 to 3. It is observed that connections with 1 or 2 bolt rows failed by bearing failure of the bolt hole in the timber plate. However, the failure mode changed to timber splitting when there were 3 bolt rows as shown in Fig. 4(c). Splitting failure was brittle and occurred suddenly without warning before the failure. Connections with steel plates also showed similar failure modes as shown in Fig. 4(d).

For the specimens in the bolt column number group, they all had the same bolt diameter of 10 mm and the number of columns varied from 1 to 3. It is observed that connections with 1 bolt column failed by bearing failure of the bolt hole in the timber plate. However, the failure mode changed to timber splitting when there were 2 or 3 bolt columns as shown in Fig. 4(e). Splitting failure was brittle and occurred suddenly without warning before the failure. The connections were loaded after the initial splitting failure and the bolts gradually embedded in the holes. Connections with steel plates also showed similar failure modes as shown in Fig. 4(f).

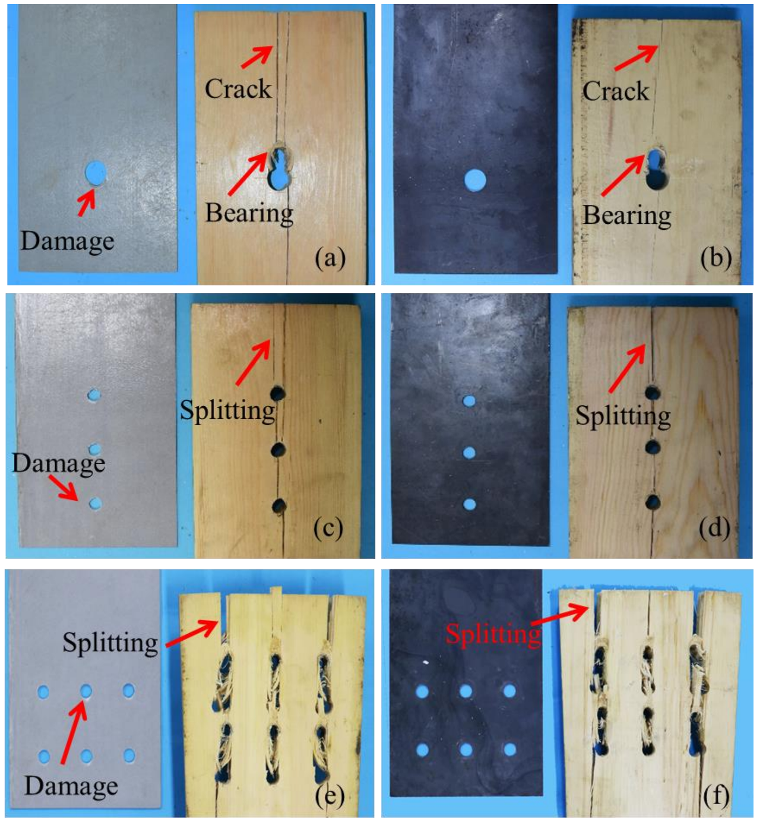

Fig. 4. Typical failure modes of specimens in static tension tests considering the effects of (a, b) bolt diameter, (c, d) number of bolt rows, (e, f) number of bolt columns

3.2. Failure loads

The failure loads of all specimens are listed in Table 3. For the bolt diameter group, when the bolt diameter was 10 mm, 14 mm and 18 mm, the failure load of the specimen was 6.64kN, 13.49kN and 13.01kN respectively. It seems that the failure load could increase significantly when the bolt diameter increased from 10 mm to 14 mm. However, increasing the bold diameter was not effective to improve the failure load when the bolt diameter was larger than 14 mm. This might be related to the bearing failure mode. The failure load was dependent on the bearing strength of the timber bolt hole, which decreased with increase of bolt diameter.

For the bolt row number group, the failure load is 10.63 kN, 17.55 kN and 20.94 kN for 1, 2 and 3 bolt rows, respectively. For the bolt column number group, the failure load is 17.55 kN, 27.78 kN, and 36.96 KN for 1, 2 and 3 bolt columns (corresponding to 2, 4, and 6 bolts), respectively. Therefore, there is an obvious increasing trend of failure load with the increase of bolt numbers.

Table 3. Experimental results of GFRP-timber bolted connections under static loading

Specimen	$\boldsymbol{F_1}$ (kN)	$\boldsymbol{F_2}$ (kN)	$\boldsymbol{F_a}$ (kN)	**Failure mode**
G-D10	6.80	6.48	6.64	Timber bearing
G-D14	12.60	14.39	13.49	GFRP bearing
G-D18	12.95	13.06	13.01	Timber bearing
S-D18	11.49	14.61	13.05	Timber bearing
G-N1	11.14	10.13	10.63	Timber bearing
G-N2	15.62	19.47	17.55	Timber splitting
G-N3	21.11	20.76	20.94	Timber splitting
S-N3	26.99	25.70	26.34	Timber splitting
G-M1	15.62	19.47	17.55	Timber splitting
G-M2	30.49	25.06	27.78	Timber splitting
G-M3	40.16	33.75	36.96	Timber splitting
S-M3	37.10	29.84	33.47	Timber splitting

Note: F_1 *and* F_2 is the bearing capacity of two specimens with the same bolt layout; F_a is the average bearing capacity of the specimens.

4. Experimental Results of Fatigue Tests

In the fatigue testing, the fatigue life N_f is defined as the number of load cycles before the failure of specimen. The fatigue ratio R is defined as the ratio of the maximum fatigue load F_{max} divided by the failure load F_a of the specimen. In this study, two load ratios of 0.5 and 0.8 were selected.

4.1. Failure modes

Typical failure modes of specimens in fatigue testing are presented in Fig. 5. Both specimens with GFRP plates and steel plates are compared. Specimens with a load ratio of 0.5 did not fail after 2 million cycles so only specimens with a load ratio of 0.8 are presented.

For the specimens in the bolt diameter group, they failed by shear off failure of the timber plate as shown in Fig. 5(a), i.e. a strip of timber in front of the bolt was pushed out. Specimens with steel plates showed similar shear off failure as shown in Fig. 5(b). It can be seen that the type of loading may change the failure mode of connection, i.e. from bearing failure under static loading to shear off failure under fatigue loading.

For the specimens in the bolt row number group, two failure modes were observed including bearing failure and shear off failure. When the connections had 1 or 2 bolts, they failed by bearing failure. However, when the connections had 3 bolts, shear off failure occurred as shown in Fig. 5(c). Specimens with steel plates showed similar shear off failure as shown in Fig. 5(b).

For the specimens in the bolt column number group, two failure modes were observed including bearing failure and timber splitting failure. When the connections had 1 column of bolts, they failed by bearing failure. When the connections had 2 or 3 columns of bolts, they failed by timber splitting failure as shown in Fig. 5(e). Specimens with steel plates showed similar timber splitting failure as shown in Fig. 5(f).

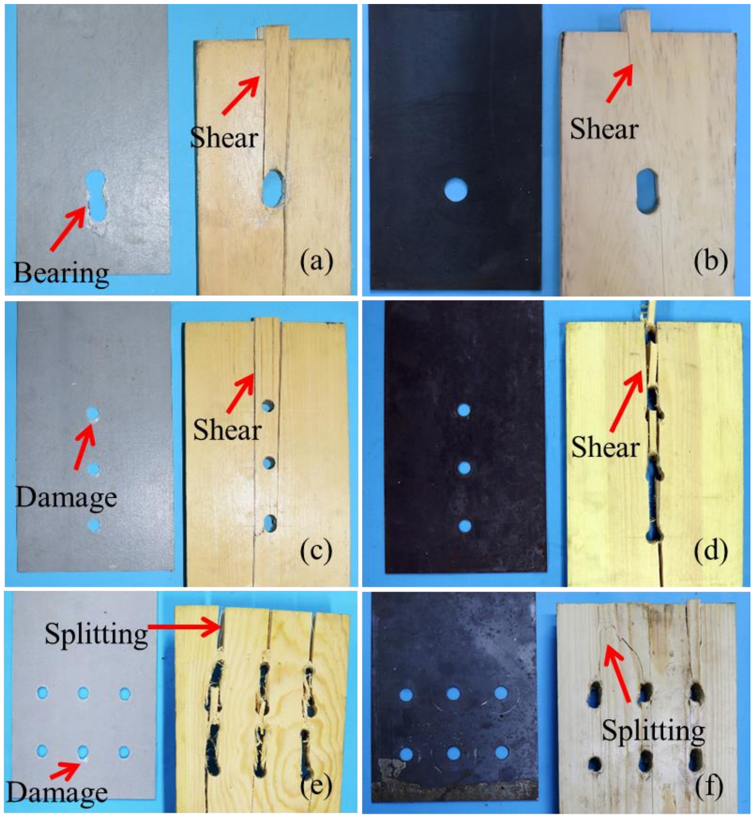

Fig. 5. Typical failure modes of specimens in fatigue tests considering the effects of (a, b) bolt diameter, (c, d) number of bolt rows, (e, f) number of bolt columns

4.2. Fatigue lives

The fatigue lives of all specimens with a load ratio of 0.8 are presented in Table 4. For the specimens in the bolt diameter group, the average fatigue life 1796 and 22 for the bolt diameter of 14 mm and 18 mm respectively. Connection with bolt diameter of 10 mm did not failure after 2 million cycles. It seems that the fatigue life decreases significantly with the bolt diameter. For the steel plate connection (G-D18-08) with a bolt diameter of 18 mm, its fatigue life is 59906 which is much higher than that of GFRP plate connection (S-D18-08).

For the specimens in the bolt row group, the average fatigue life is 6023, 15849 and 22,500 for 1, 2 and 3 bolts, respectively. It is obvious that the fatigue life of GFRP-timber connections increases with the number of bolts. Interestingly, the steel plate connection with 3 bolts (S-N3-08) has a fatigue life of 179 which is much less than the corresponding GFRP plate connection (G-N3-08, 22500).

For the specimens bolt column group, the average fatigue life is 15849, 955 and 3880 for 1, 2 and 3 bolt columns, respectively. The steel plate connection with 3 bolt columns (S-M3-08) has a fatigue life of 111466 which is much higher than the corresponding GFRP plate connection (G-M3-08, 3880).

It seems that some steel connections have higher fatigue life than corresponding GFRP connections while others show a reverse relationship. This is because the steel connections may have different absolute fatigue loading from the GFRP connections though they have the same load ratio. The absolute fatigue load depends on the static failure load of the connection.

Table 4. Fatigue test results (R=0.8) of GFRP-timber bolted connections

Specimen	$N_{f,0.8,1}$	$N_{f,0.8,2}$	$N_{f,0.8,a}$	**Failure mode**
G-D10-08	＞2,000,000	＞2,000,000	＞2,000,000	Not failed
G-D14-08	335	3257	1796	Timber shear off
G-D18-08	26	19	22	Timber shear off
S-D18-08	58903	60909	59906	Timber shear off
G-N1-08	9210	2836	6023	Timber bearing
G-N2-08	31667	32	15849	GFRP bearing
G-N3-08	14512	30489	22500	Timber shear off
S-N3-08	325	34	179	Timber shear off

G-M1-08	31667	32	15849	GFRP bearing
G-M2-08	1851	59	955	Timber splitting
G-M3-08	795	6965	3880	Timber splitting
S-M3-08	52651	170281	111466	Timber shear off

Note: $N_{f,0.8,1}$ and $N_{f,0.8,2}$ is the fatigue life of two specimens with the same bolt layout; $N_{f,0.8,a}$ is the average fatigue life of the specimens.

4.3. Stiffness degradation

The stiffness of the specimens in the bolt diameter group is plotted against the normalized fatigue life in Fig. 6. Here, the joint stiffness (K_i), is defined as the load range ($F_{max,i}$-$F_{min,i}$) in a specific fatigue load cycle (i.e. ith cycle) divided by the cyclic displacement increment ($\delta_{max,i}$-$\delta_{min,i}$) in that corresponding cycle, i.e. $Ki=(F_{max,i}-F_{min,i})/(\delta_{max,i}-\delta_{min,i})$. The normalized fatigue life is calculated using the number of cycles divided by the fatigue life of the connection, i.e. r = i/N. For specimens with a load ratio of 0.8, the stiffness is higher with larger bold diameter. GFRP plate connections exhibit fluctuations throughout their entire fatigue lives. This is due to the progressive damage at the bolt holes. The crushed timber debris fill the gaps in the connection resulting in increase in stiffness, while the failure of timber holes see decrease in stiffness. This crushing and filling effects exist throughout the entire fatigue life. It is also clear that the steel plate connection has a much higher stiffness than the corresponding GFRP connection.

Similar results are observed for connections with a load ratio of 0.5, i.e. fluctuation of stiffness due to crushing and filling effects. However, the steel connection has similar stiffness to the corresponding GFRP connection. Another observation in Fig. 6 is that, most specimens with 0.8 load ratio have relatively higher stiffness than the corresponding connections with 0.5 load ration. This is because 0.8 load ratio will generate higher dynamic effect because the same fatigue frequency was adopted for all specimens. The load was increased much faster to the target with a higher load ration resulting in a greater dynamic effect.

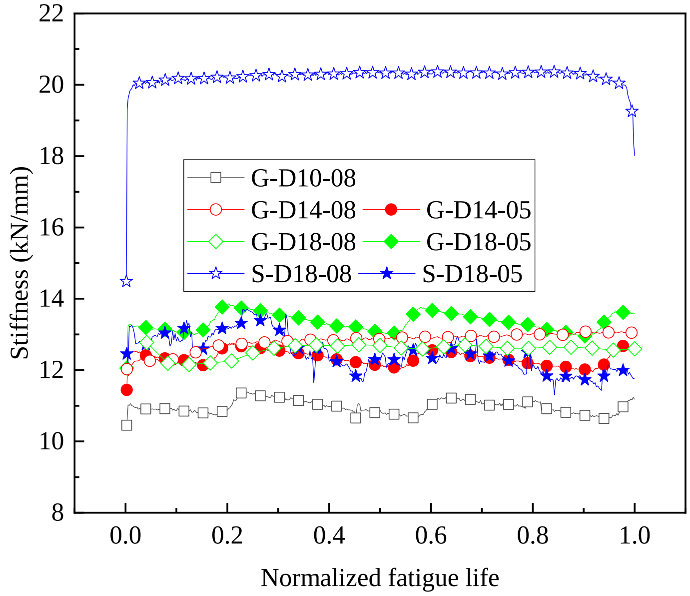

Fig. 6. Stiffness degradation curves of the bolt diameter group

The stiffness curves of the specimens in the bolt row number group are presented in Fig. 7. Regardless of the load ratio, all specimens show a positive relationship between the stiffness and the number of bolts, i.e. connections with more bolts have higher stiffness. Fluctuations are also observed for most specimens due to the same crushing and filling effects. Again, the steel plate connection has a much higher stiffness than the corresponding GFRP plate connection. Specimens with a load ratio of 0.8 show higher stiffness than those with a load ratio of 0.5 due to the dynamic effect.

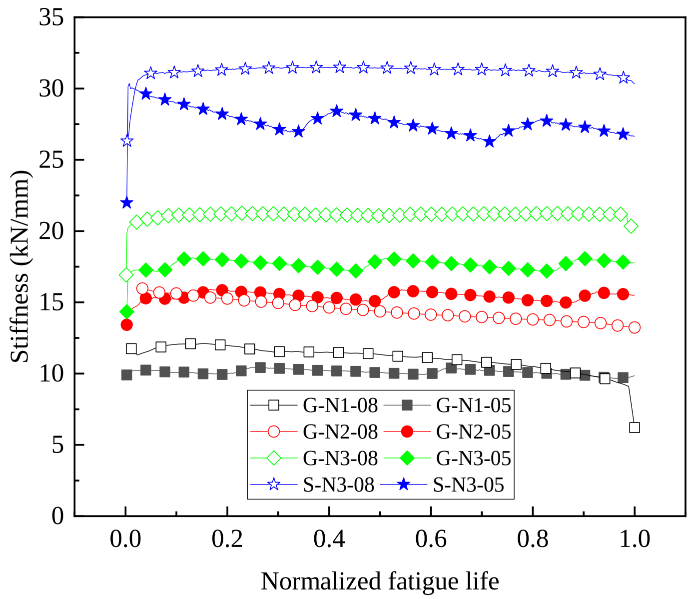

Fig. 7. Stiffness degradation curves of the bolt row number group

The stiffness curves of the specimens in the bolt column number group are presented in Fig. 8. Again, the stiffness of connection is positively correlated with the bolt number, i.e. connections with more bolts have greater stiffness, regardless of the load ratio. Fluctuations are also observed for most specimens due to the same crushing and filling effects. Specimens with a load ratio of 0.8 see some decrease in stiffness before final failure while those with a load ratio of 0.5 maintain almost constant throughout the fatigue life. Again, the steel plate connection has a much higher stiffness than the corresponding GFRP plate connection. Specimens with a load ratio of 0.8 show higher stiffness than those with a load ratio of 0.5 due to the dynamic effect.

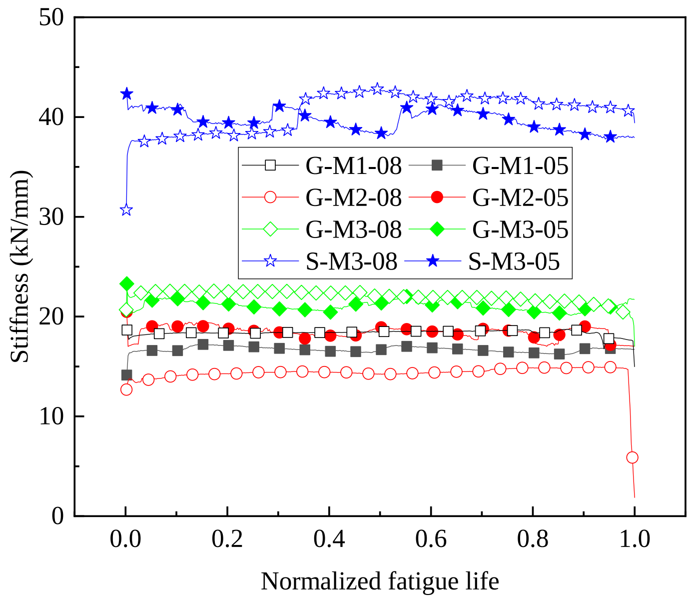

Fig. 8. Stiffness degradation curves of the bolt column number group

5. Experimental Results of Residual Bearing Capacity Tests after Fatigue Loading

5.1. Failure modes

The specimens with a load ratio of 0.5 did not fail in the fatigue tests, so they were tensioned to failure to assess their residue static load bearing capacities. Typical failure modes are presented in Fig. 9. Both specimens with GFRP plates and steel plates are compared.

For the specimens in the bolt diameter group, they exhibited hole bearing failure of the GFRP plates as shown in Fig. 9(a). This is different from the static tensile testing which is timber hole bearing failure as shown in Fig. 4(a). This may be due to the cumulative damage in the GFRP holes during the fatigue testing as seen in Fig. 5(a). After GFRP bearing failure, the connections were able to carry some load and eventually failed by the shear off of the timber plate, i.e. the bolt pushed a strip of timber out of the timber plate as shown in Fig. 9(b).

For the specimens in the bolt row number group, two failure modes were observed including GFRP bearing failure and timber shear off failure. Connections with 1 or 2 bolts failed by GFRP bearing failure while those with 3 bolts failed by timber shear off failure as shown in Fig. 9(c). Steel plate connection with 3 bolts also showed timber shear off failure as shown in Fig. 9(d) which is similar to the corresponding GFRP connection.

For the specimens in the bolt column number group, two failure modes were also observed, namely, GFRP hole bearing failure and timber plate shear off failure. Connections with 1 bolt column failed by GFRP hole bearing failure, while those with 2 or 3 bolt columns failed by timber shear off failure as shown in Fig. 9(e). Steel plate connection with 3 bolt columns also showed timber shear off failure as shown in Fig. 9(f) which is similar to the corresponding GFRP connection.

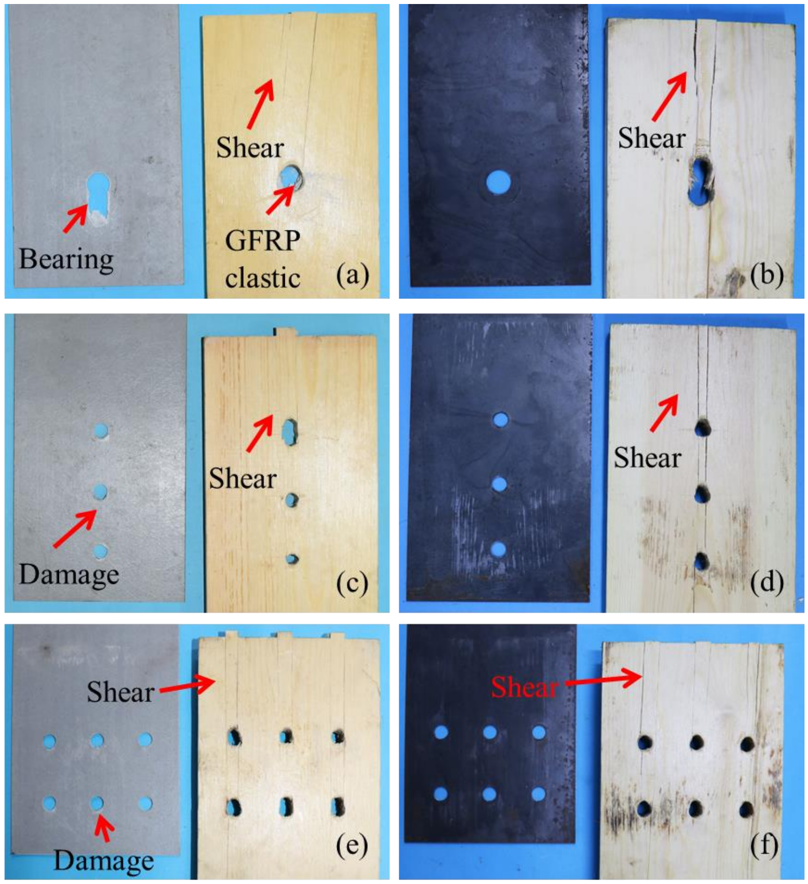

Fig. 9. Typical failure modes of specimens under static loading for the assessment of the residual load bearing capacity considering the effects of (a, b) bolt diameter, (c, d) number of bolt rows, (e, f) number of bolt columns

5.2. Load-displacement curves

The load-displacement curves of residual bearing capacity test for all specimens in the bolt diameter group are shown in Fig. 10. The specimens in the static tension testing are also presented for comparison purpose. At the initial stage, the tensile load increases linearly with the displacement, and the slope of the curve increases slightly with the increase of bolt diameter. After the peak load, the curve drops a bit and then fluctuates at a certain level. The tests stopped when the displacement reached 20 mm.

For specimens in static testing, they experienced timber bolt hole bearing failure (Fig. 4a), while for specimens in residue capacity testing, they showed GFRP hole bearing failure (Fig. 9a). These are progressive failure modes which is the reason for the fluctuations of the load-displacement curves in Fig. 10. It is also observed that the slope of the curves of the specimens in the residue capacity testing is generally greater than the slope of the curves of the specimens in the static testing. That means specimens see increase in stiffness in the bearing capacity testing. This is also because of the crushing and filling effect in the fatigue tests. The debris filled the gaps in the connections which made them tighter and more compact, leading to increased stiffness.

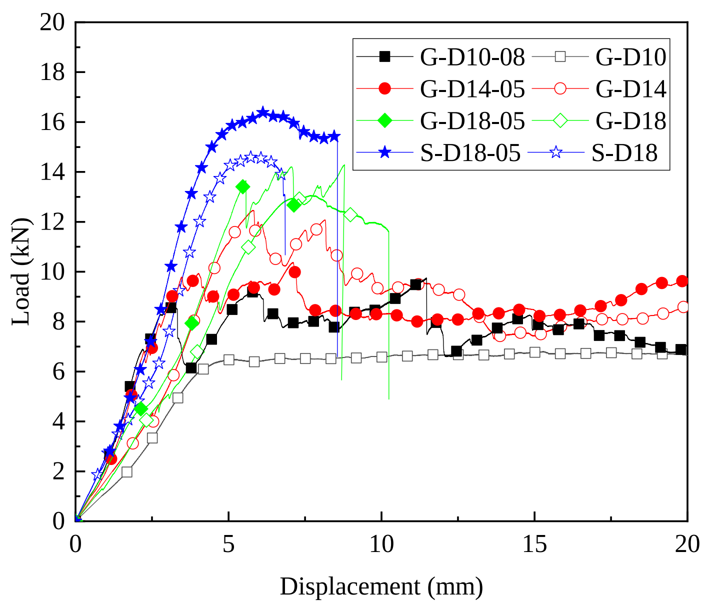

Fig. 10. Load-displacement curves of specimens in the bolt diameter group

The load-displacement curves of residual bearing capacity test of all specimens in the bolt row number group are shown in Fig. 11. The specimens in the static tension testing are also presented for comparison purpose. The curves can be divided into two patterns. The first pattern is curve fluctuation after the peak. This pattern is seen for connection with

1 or 2 bolts. This is because these connections failed by hole bearing failure (Figs. 4, 9), which is a progressive failure mode. The second pattern is curve drop quickly after the peak. This pattern is seen for connections with 3 bolts which failed by a sudden shear off failure. In addition, the stiffness (curve slope) increases with the number of bolts. It is also observed that connections in the residue capacity testing have greater stiffness than the corresponding connections in the static testing. The reason is similar, i.e. crushing and filling effect in the fatigue tests making the connections more compact and stiff.

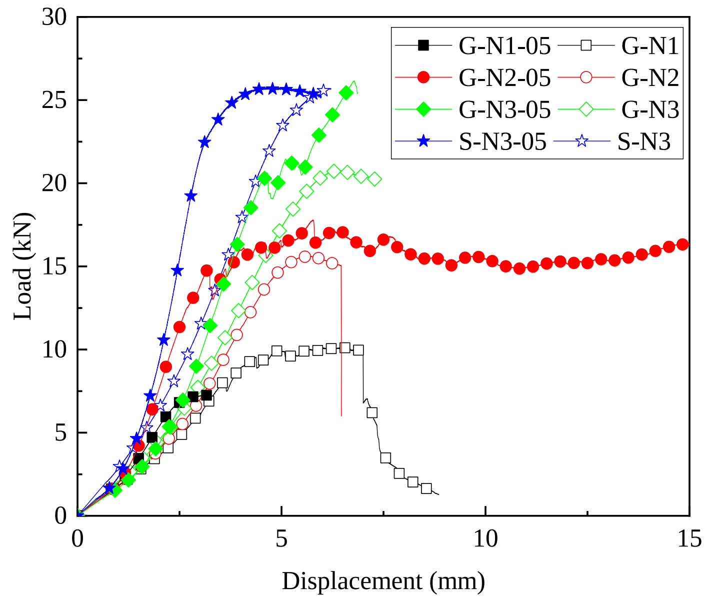

Fig. 11. Load-displacement curves of specimens in the bolt row number group

Residual bearing capacity test load-displacement curves of all specimens in bolt column number group are shown in Fig. 12. The specimens in the static tension testing are also presented for comparison purpose. Again, three observations can be made. Firstly, two curve patterns with one showing fluctuation after peak and the other showing quick drop after peak. The first pattern is related to the progressive hole bearing failure of connections with 1 bolt column. The other pattern is related to the shear off failure of the connections with 2 or 3 bolt columns. The second observation is that the stiffness of the specimen is proportional to the number of bolt columns. Thirdly, due to the same crushing and filling effect, connections in the residue capacity testing have greater stiffness than the corresponding connections in the static testing.

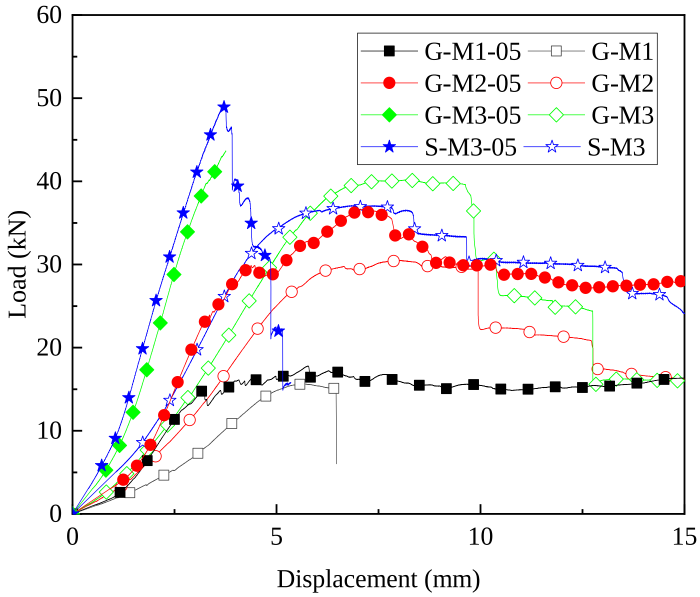

Fig. 12. Load-displacement curves of specimens in the bolt column number group

5.3. Residual load bearing capacities

The residual load bearing capacities after fatigue loading are listed in Table 5. They are also compared with the static bearing capacities without fatigue loading effect in Fig. 13. It can be observed from Fig. 13 that the residual bearing capacities of specimens in bolt diameter group and bolt row number group are close to their static bearing capacities, indicating that the fatigue load has very limited effect on the bearing capacities of specimens. For the specimens in the bolt column number group, when the number of bolt columns is 1 or 2, the bearing capacities do not change much before and after fatigue loading. But when the number of bolt columns is 3, the residual bearing capacity of the connection is obviously higher than its static bearing capacity. This may be because, after two million fatigue cycles, the forces carried by the bolts are redistributed in the connection with 3 columns of bolts. The six bolts carry the load more uniformly reducing the group effect of the connection, and each bolt is fully involved in force transfer. Finally, the bearing capacity of the connection with 3 columns of bolts was improved after fatigue loading.

Table 5. Test results of residual bearing capacity

Specimen	$N_{f,0.5}$	$F_{f,1}/F_a$	$F_{f,2}/F_a$	$F_{f,a}/F_a$	**Failure mode**
G-D14-05	＞2,000,000	95.18%	103.48%	99.33%	GFRP bearing
G-D18-05	＞2,000,000	108.61%	109.84%	109.23%	Timber shear off
S-D18-05	＞2,000,000	125.59%	115.10%	120.35%	Timber shear off
G-N1-05	＞2,000,000	68.20%	81.56%	74.88%	Timber shear off
G-N2-05	＞2,000,000	107.58%	90.48%	99.03%	GFRP bearing
G-N3-05	＞2,000,000	124.88%	144.32%	134.60%	Timber shear off
S-N3-05	＞2,000,000	97.80%	89.52%	93.66%	Timber shear off
G-M1-05	＞2,000,000	107.58%	90.48%	99.03%	GFRP bearing
G-M2-05	＞2,000,000	92.02%	132.07%	112.05%	Timber shear off
G-M3-05	＞2,000,000	150.00%	118.20%	134.10%	Timber shear off
S-M3-05	＞2,000,000	182.24%	146.49%	164.37%	Timber shear off

Note: $N_{f,0.5}$ is the fatigue life of the specimen; $F_{f,1}$ and $F_{f,2}$ is the residual bearing capacity of two specimens with the same bolt layout; $F_{f,a}$ is the average residual bearing capacity of the specimens.

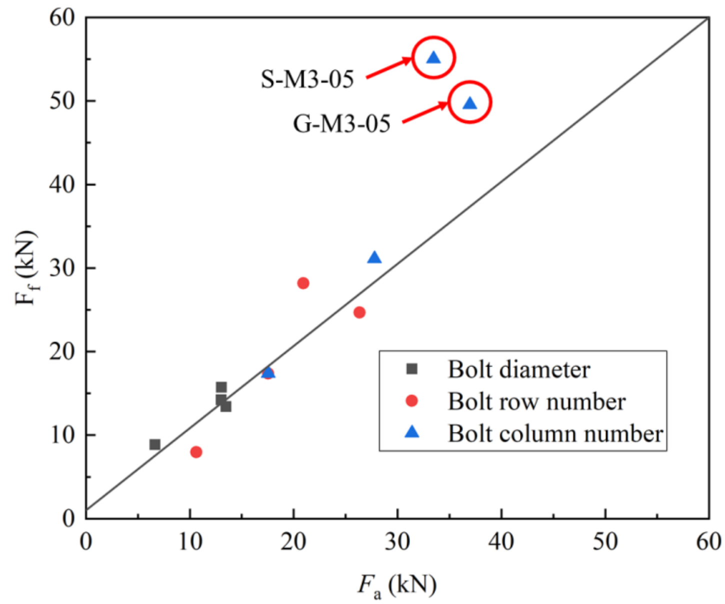

Fig. 13. Comparison of residual and static bearing capacities

6. Conclusions

Considering the durability issue due to corrosion of steel plate in timber bolted connections, this paper proposed a GFRP-timber bolted connection, and experimentally investigated its tensile and fatigue performances. The effects of bolt diameter, bolt row number and bolt column number were analyzed. According to the experimental results of this paper, the following conclusions can be drawn:

(1) GFRP plate connections showed similar or even greater static bearing capacities comparing with the conventional steel plate connections.

(2) GFRP plate connections generally showed shorter fatigue lives comparing with the conventional steel plate connections under the same fatigue load ratio. However, it should be noted that the actual fatigue performances of both GFRP and steel connections should also be compared using the same absolute fatigue loads, which was not conducted in this paper.

(3) The fatigue life of the GFRP plate connection is negatively correlated with bolt

diameter and positively correlated with the number of bolts. GFRP plate connections with a fatigue load ratio of 0.5 did not fail after 2 million cycles.

(4) For connections in static testing, timber hole bearing failure and timber splitting failure were observed. For connections in fatigue testing, GFRP hole bearing failure and timbe shear off failure were observed. For connections in residue capacity testing, GFRP hole bearing failure and timbe shear off failure were also observed.

(5) Fatigue loading had effect on the failure mode of the GFRP plate connection. It incurred cumulative damages in the GFRP plates resulting in the hole bearing failure in the residue capacity testing. Fatigue damage also made it more likely to have brittle timber shear off failure.

(6) Fatigue loading had effect on the static mechanical properties of the GFRP plate connection. Materials around the holes got crushed and debris filled the gaps of the connection during fatigue loading. This lead to increase in static stiffness of the connection. The static bearing capacity may also be enhanced.

The results reported in this paper demonstrate the significance and importance of investigating the static and fatigue performances of GFRP-timber bolted connections. It also highlights the importance of properly accounting for the group effect of the bolts in the design. However, it should be mentioned that the above conclusions are based on test results of two replicate samples which may not provide sufficient data from a statistical point of view despite the consistency of the results. It is therefore recommended that comprehensive experimental tests with more representative replicate samples should be conducted to ascertain the preliminary results reported in the current paper. In addition, it should be noted that adhesively bonded connection can have better performance with improved stiffness and less stress concentration due to bolt holes. It is recommended that future studies investigate the adhesively bonded connection and compare the results in this study. This is to investigate how better performance of the GFRP-timber connection can be achieved.

Acknowledgments

The authors gratefully acknowledge the financial support provided by the National Science Foundation of China (51978025). Mr. Menglong Shao and Ms. Yue Ding is acknowledged for their assistance of conducting the experimental tests at Beihang University.

Data Availability Statement

The raw/processed data required to reproduce these findings cannot be shared at this time as the data also forms part of an ongoing study.

REFERENCES

[1] Li JH, Rismanchi B, Ngo T. Feasibility study to estimate the environmental benefits of utilising timber to construct high-rise buildings in Australia. Building And Environment. 2019;147:108-20.

[2] Skullestad JL, Bohne RA, Lohne J. High-rise Timber Buildings as a Climate Change Mitigation Measure – A Comparative LCA of Structural System Alternatives. Energy Procedia. 2016;96:112-23.

[3] Awaludin A, Hirai T, Hayashikawa T, Sasaki Y. Load-carrying capacity of steel-to-timber joints with a pretensioned bolt. Journal of Wood Science. 2008;54:362-8.

[4] Gattesco N, Toffolo I. Experimental study on multiple-bolt steel-to-timber tension joints. Materials & Structures. 2004;37:129-38.

[5] Jensen JL, Quenneville P. Experimental investigations on row shear and splitting in

bolted connections. Construction and Building Materials. 2011;25:2420-5.

[6] Kharouf N, McClure G, Smith I. Postelastic behavior of single- and double-bolt timber connections. Journal of Structural Engineering. 2005;131:188-96.

[7] Santos CL, De Jesus AMP, Morais JJL, Lousada JLPC. Quasi-static mechanical behaviour of a double-shear single dowel wood connection. Construction and Building Materials. 2009;23:171-82.

[8] Quenneville JHQ, Mohammad M. On the failure modes and strength of steel-wood-steel bolted timber connections loaded parallel-to-grain. Canadian Journal of Civil Engineering. 2000;27:761-73.

[9] Mohammad M, Quenneville JHP. Bolted wood-steel and wood-steel-wood connections: verification of a new design approach. Canadian Journal of Civil Engineering. 2001;28:254-63.

[10] Singh PM, Anaya A. Effect of wood species on corrosion behavior of carbon steel and stainless steels in black liquors. Corrosion Science. 2007;49:497-509.

[11] Zelinka SL, Stone DS. The effect of tannins and pH on the corrosion of steel in wood extracts. Materials And Corrosion-Werkstoffe Und Korrosion. 2011;62:739-44.

[12] Harries KA, Guo Q, Cardoso D. Creep and creep buckling of pultruded glass-reinforced polymer members. Composite Structures. 2017;181:315-24.

[13] Liu T, Yang JQ, Feng P, Harries KA. Determining rotational stiffness of flange-web junction of pultruded GFRP I-sections. Composite Structures. 2020;236.

[14] Xiong Z, Liu Y, Zuo Y, Xin H. Experimental evaluation of shear behavior of pultruded GFRP perforated connectors embedded in concrete. Composite Structures. 2019;222.

[15] Shekarchi M, Oskouei AV, Raftery GM. Flexural behavior of timber beams

strengthened with pultruded glass fiber reinforced polymer profiles. Composite Structures. 2020;241.

[16] Corradi M, Vo TP, Poologanathan K, Osofero AI. Flexural behaviour of hardwood and softwood beams with mechanically connected GFRP plates. Composite Structures. 2018;206:610-20.

[17] Liu T, Vieira JD, Harries KA. Lateral torsional buckling and section distortion of pultruded GFRP I-sections subject to flexure. Composite Structures. 2019;225.

[18] Zhang L, Liu W, Wang L, Ling Z. On-axis and off-axis compressive behavior of pultruded GFRP composites at elevated temperatures. Composite Structures. 2020;236.

[19] Ghadimi B, Russo S, Rosano M. Predicted mechanical performance of pultruded FRP material under severe temperature duress. Composite Structures. 2017;176:673-83.

[20] Grammatikos SA, Jones RG, Evernden M, Correia JR. Thermal cycling effects on the durability of a pultruded GFRP material for off-shore civil engineering structures. Composite Structures. 2016;153:297-310.

[21] Yan Y, Wen WD, Chang FK, Shyprykevich P. Experimental study on clamping effects on the tensile strength of composite plates with a bolt-filled hole. Composites Part A: Applied science and manufacturing. 1999;30(10):1215-29.

[22] Gray PJ, McCarthy CT. A global bolted joint model for finite element analysis of load distributions in multi-bolt composite joints. Composites Part B: Engineering. 2010;41:317-25.

[23] Starikov R, Schon J. Quasi-static behaviour of composite joints with countersunk composite and metal fasteners. Composites Part B: Engineering. 2001;32:401-9.

[24] Starikov R, Schon J. Quasi-static behaviour of composite joints with protruding-head

bolts. Composite Structures. 2001;51:411-25.

[25] Feo L, Marra G, Mosallam AS. Stress analysis of multi-bolted joints for FRP pultruded composite structures. Composite Structures. 2012;94:3769-80.

[26] Ascione F. A preliminary numerical and experimental investigation on the shear stress distribution on multi-row bolted FRP joints. Mechanics Research Communications. 2010;37:164-8.

[27] Wu C, Feng P, Bai Y. Comparative study on static and fatigue performances of pultruded GFRP joints using ordinary and blind bolts. Journal of Composites for Construction. 2014;19:04014065.

[28] Lawlor VP, McCarthy MA, Stanley WF. An experimental study of bolt–hole clearance effects in double-lap, multi-bolt composite joints. Composite Structures. 2005;71:176-90.

[29] Persson E, Eriksson I. Fatigue of multiple-row bolted joints in carbon/epoxy laminates: Ranking of factors affecting strength and fatigue life. International Journal of Fatigue. 1999;21:337-53.

[30] Starikov R, Schön J. Experimental study on fatigue resistance of composite joints with protruding-head bolts. Composite Structures. 2002;55:1-11.

[31] Abdelkerim DSE, Wang X, Ibrahim HA, Wu Z. Static and fatigue behavior of pultruded FRP multi-bolted joints with basalt FRP and hybrid steel-FRP bolts. Composite Structures. 2019;220:324-37.

[32] Abendroth RE, Wipf TJ. Cyclic load behavior of bolted timber joint. Journal of Structural Engineering. 1989;115:2496-510.

[33] Jockwer R, Fink G, Köhler J. Assessment of the failure behaviour and reliability of timber connections with multiple dowel-type fasteners. Engineering Structures.

2018;172:76-84.

[34] Yurrita M, Cabrero JM, Quenneville P. Brittle failure in the parallel-to-grain direction of multiple shear softwood timber connections with slotted-in steel plates and dowel-type fasteners. Construction and Building Materials. 2019;216:296-313.

[35] CEN. Eurocode 5: Design of timber structures - Part 1-1: General Common rules and rules for buildings. Europe: CEN; 2004.

[36] Jorissen A. Double shear timber connections with dowel type fasteners. Heron. 1999;44:163-86.

[37] Wu C, Zhang Z, Tam LH, Feng P, He L. Group effect of GFRP-timber bolted connections in tension. Composite Structures. 2020:113637.

[38] ASTM D 3039 Standard test method for tensile properties of polymer matrix composite materials. West Conshohocken: ASTM International; 2017.

[39] ASTM D 3518 Standard test method for in-plane shear response of polymer matrix composite materials by tensile test of a ±45° laminate. West Conshohocken: ASTM International; 2018.

[40] ASTM D 3171 Standard test methods for constituent content of composite materials. West Conshohocken: ASTM International; 2015.

[41] ASTM D 5764 Standard test method for evaluating dowel-bearing strength of wood and wood-based products. West Conshohocken: ASTM International; 2013.

[42] ASTM D 4442 Standard test methods for direct moisture content measurement of wood and wood-based materials. West Conshohocken: ASTM International; 2016.

[43] ASTM D 2395 Standard test methods for density and specific gravity (relative density) of wood and wood-based materials. West Conshohocken: ASTM International; 2017.

[44] ASTM A 307: Standard specification for carbon steel bolts, studs, and threaded rod 60000 PSI tensile strength. West Conshohocken: ASTM International; 2014.

[45] Dittenber DB, Rao HVSG. Fatigue equation considerations for the American Society of Civil Engineers pre-standard for load and resistance factor design of pultruded fiber-reinforced polymer structures. Journal of Composite Materials. 2013;47:1943-9.